Anodic Processes on a Galena (PbS) Electrode in the Presence of *n*-Butyl Xanthate Studied FTIR-Spectroelectrochemically

I. V. Chernyshova†

St. Petersburg State Technical University, Polytechnicheskaya 29, 195251 St. Petersburg, Russia

Received: March 19, 2001; In Final Form: June 9, 2001

Anodic reactions on a galena (PbS) electrode in solutions of *n*-butyl xanthate (X) were studied in situ using attenuated total reflection/FTIR spectroscopy within the −0.5 to +0.7 V potential range in deaerated borate buffer (pH 9.2). It was confirmed that at the first stage X is adsorbed with charge transfer (chemisorbed). It was found that *n*-butyl dixanthogen, $(X)_2$, is formed at the reversible potential for the $X^-/(X)_2$ pair, independently of the X concentration. The appearance of dixanthogen makes the surface most hydrophobic, which can be followed from the changes in the water spectrum. Otherwise, the mechanisms of the X adsorption at high and low concentrations have differences. At a concentration of 10^{-3} M, oxidative decomposition of galena and adsorbed xanthate is inhibited by the X chemisorption, which is followed by the formation of lead xanthate, $Pb(X)_2$, and $(X)_2$. At 8×10^{-5} M, bulk $Pb(X)_2$ is formed by the precipitation mechanism. At higher applied potentials first $Pb(X)_2$ transforms into $Pb(OH)_2$. Afterward $(X)_2$ decomposes into a dimer of monothiocarbonate, while galena decomposes into lead sulfite and lead thiosulfate. The possible reactions for these processes were suggested. The results were correlated with the literature data on galena flotation.

Introduction

Oxidation of organic molecules at semiconducting electrodes is of interest not only for fundamental science but also from the viewpoint of numerous technological applications such as electrocatalyzed synthesis, corrosion inhibition, flotation, etc.[1] Alkyl xanthates (dithiocarbonates) $ROCS_2^-$ have been used industrially as collectors (hydrophobizing agents) for flotation of sulfides since 1925. Since that time, the mechanism of the xanthate action has been studied, a variety of hypotheses being put forward (for reviews, see refs 2−7). Briefly, all the models can be classified into two categories: chemical and electrochemical. Attachment of the collector by replacement of surface oxidation products[8,9,10] or lattice ions,[11,12] adsorption,[13,14] and coordination[15] are assigned to the *chemical mechanism*. This concept, however, neglects the formation of dixanthogen $(ROCS_2)_2$ (the most hydrophobic derivative of xanthate) and fails to explain poor floatabilities of heavy oxidized lead and copper sulfides (when the solubility product of the metal xanthate is significantly exceeded[16]) and poor floatability of slightly oxidized sphalerite, which is an insulator. According to the *electrochemical (mixed-potential) mechanism*,[17] the xanthate adsorption on semiconducting sulfides is accompanied by charge transfer within a particle from its cathodic patch, at which oxygen is reduced, to the anodic one, at which xanthate anion interacts with the sulfide. This mechanism is more general, involving the chemical mechanisms as the specific case.[2−4]

The dual (chemical and electrochemical) reactivity of the semiconducting sulfides in the pulp has resulted in IR spectroscopic studies having been historically conducted in two ways: under the conditions when the thermodynamics and kinetics of the reaction (the energy profile at the interface) are controlled either chemically or potentiostatically. The surface potential is controlled chemically by varying the redox couple in the solution. This approach is more closely related to the plant practice, but the studies of the surface reactions under chemical control are complicated by reactions between the redox agents and the surface. Potentiostatic control is "cleaner", more flexible, and informative. Easily manipulating the interfacial potential difference by a potentiostat, one can model all states of the surface reactivity and, therefore, quantify the surface layer characteristics (composition and structure) in terms of the mineral potential, which is of substantial importance for controlling the flotation process.

The anodic reactions at semiconducting sulfides at controlled potential have been studied intensively by using classical electrochemical methods,[2−4,18−22] the UV−vis solution depletion method, and IR and XPS spectroscopy (for a review, see ref 4), the system "galena−xanthate" being studied the most intensively. At least four forms of xanthate have been found or postulated for galena: chemisorbed radical, physisorbed xanthate, metal xanthate complex, dixanthogen, and monothiocarbonate (MTC) (or the dimer of MTC). Chemisorbed xanthate $(X = ROCS_2^-)$

$$X^- + h^+ \rightleftharpoons X_{ads} \quad (1)$$

where h^+ stands for hole, has been initially suggested[4,20] to explain the prepeak in voltammograms (at −0.05 V (SHE) in 0.001 M *n*-butyl xanthate solution[3]). However, this species has been doubted on the basis of the chronoamperometric,[21] interfacial impedance,[22] and chemical equilibrium[14] data. On the other hand, the diffuse reflectance (DRIFT) spectra[23] of the galena powder conditioned with ethyl xanthate solutions even of concentration as high as 10^{-3} M exhibit only the bands of lead xanthate, $Pb(X)_2$. According to thermodynamics, the anodic reaction for the formation of this compound can be

$$PbS + 2X^- \rightleftharpoons Pb(X)_2 + S^\circ + 2e^{2,3,24-27} \; (E^\circ = -0.186 \text{ V}) \quad (2)$$

† E-mail: Irina.Chernyschova@pobox.spbu.ru. Fax: +7 (812) 428-5712.

10.1021/jp011026v CCC: $20.00
Published on Web 08/07/2001

$$2PbS + 4X^- + 3H_2O \rightleftharpoons 2Pb(X)_2 + S_2O_3^{2-} + 6H^+ + 8e^{7,26,28} \quad (E^\circ = +0.170\ V^7) \quad (3)$$

(in parentheses are given the standard potentials for *n*-butyl xanthate). As shown in our previous work,[29] the anodic decomposition of galena starts with incongruent dissolution

$$PbS + 2xh^+ \rightleftharpoons Pb_{1-x}S + xPb^{2+} \quad (4a)$$

Therefore, one can expect that bulk $Pb(X)_2$ can form under such conditions by the precipitation mechanism:

$$Pb^{2+} + 2X^- \rightleftharpoons Pb(X)_2\ (pK_{SP} = -18.87^{30}) \quad (4b)$$

Dixanthogen, $(X)_2$, is a product of the surface-mediated anodic oxidation of xanthate ions[2]

$$2X^- + 2h^+ \rightleftharpoons (X)_2\ (E^\circ = -0.08 \text{ to } -0.12\ V^{18}) \quad (5a)$$

which can involve chemisorption 1 as the initial step

$$X_{ads} + X^- \rightleftharpoons (X)_2 + e \quad (5b)$$

At the same time, dixanthogen has not been found spectroscopically at a galena surface at concentrations used in flotation ($<10^{-4}$ M) either ex situ[23,31,32] or in situ[33] yet, but has been detected by the extraction method.[3,34] The only exception is the DRIFTS of *n*-amyl xanthate adsorbed on galena wet ground at pH 11,[32,35,36] which is the specific case. On the basis of these findings, chemisorbed xanthate[3,4] and molecular lead xanthate, $Pb(X)_2$,[5,23,26,31−33] have been suggested to play the main hydrophobizing role, while it is natural to anticipate[7,18,37] that the highest floatability is provided by dixanthogen.

The observed[26] decrease in the flotation rate for galena in 2.3×10^{-5} M ethyl xanthate solution (pH 8) at ca. +0.35 V has been ascribed[26,27] to transformation of lead xanthate into lead hydroxide

$$Pb(X)_2 + 2OH^- + 2h^+ \rightleftharpoons Pb(OH)_2 + (X)_2\ (E^\circ = 0.819\ V^{18}) \quad (6)$$

Self-oxidation of galena has also been considered as a possible reaction for low[27] and even high[22,38] xanthate concentrations. At last, $Pb(X)_2$ can be decomposed with formation of hydrophilic MTC as its dimer,[32,39] and Leja[40] listed a series of reactions that could describe this process.

The uncertainties and contradictions mentioned originate from the intrinsic ambiguity of the indirect data[29] and from the fact that most of the spectroscopic information has been obtained ex situ. At the same time, it has been found that even relatively "heavy" *n*-amyl dixanthogen evaporates from the surface rather quickly in open air,[41] not to mention the UHV conditions,[42] and the dixanthogen component of the adsorbed layer is eliminated by sampling for DRIFTS.[43] Moreover, it has been established[44] that destruction of the electrical double layer with evaporating solvent can significantly alter the adsorbate structure—a characteristic which controls the wettability of the surface.

The xanthate adsorption on galena (natural PbS) has been studied in situ only by Leppinen et al.[33] According to the attenuated total reflection (ATR)/FTIR spectra reported, the only adsorption form of xanthate within the potential range from −0.25 to +0.6 V (SHE) is bulk lead xanthate. Although the intensity of the absorption bands of lead xanthate was found to follow the current density in the voltammogram, steeply increasing at 0 V, the qualitative identity of the adsorption film can hardly explain the steep increase in the contact angle and floatability at 0 V.[28] This contradiction with the indirect results[25,27] may originate from the possible artifacts due to the constructional features[43,45] of the technique of Leppinen et al. Moreover, the spectra were measured at a xanthate concentration of 1×10^{-3} M, which is much higher than the typical flotation concentration. At the same time, it is known[27] that the adsorption mechanism in this collector concentration range differs from that at low concentration.

The aim of the present work was to study in situ anodic reactions on a galena electrode in the presence of *n*-butyl xanthate at a concentration typical for flotation and to compare the results with those obtained for high concentration. The study was carried out by using the ATR technique,[46] which is free from the constructive restrictions of the technique of Leppinen et al. and has a sensitivity of 0.1 monolayer of adsorbed xanthate.

Experimental Section

In situ ATR/FTIR spectra of the galena/solution interface were measured in the spectroelectrochemical cell described in detail elsewhere.[46] Classical electrochemical equipment (potentiostat PI-50-1 and programmer PR-8, Russia) was employed in three-electrode configuration. The potential−current density dependence was measured with an *X*−*Y* recorder. The counter electrode was a Pt wire. The potentials were measured against a saturated potassium chloride electrode connected via a Luggin capillary to the cell, while all potentials reported here are converted to the standard hydrogen electrode (SHE).

The working electrode was prepared in the following way. A galena plate was cut along a (100) crystallographic plane from single-crystal galena, whose minor elements determined by mass spectrometry with an INA-3 Leybold AG instrument were Ag (3000 ppm), Sb (1200 ppm), and Sn (40 ppm). This plate was glued by using a low-melting halcogenide glass to a halcogenide glass hemicylindric internal reflection element (IRE). The working surface was wet polished successively with 1.0 and 0.3−0.05 mm alumina (Buehler) and washed thoroughly with distilled water. After that, the "glued plate−IRE" assembly was attached to the cell. On the basis of the literature data,[27,29,47] the surface oxidation products and impurities were removed and the reproducibility of the initial surface was provided by keeping the galena electrode at −0.5 V for 1 h before each experiment. Afterward, the electrode potential was increased stepwise from −0.5 V. At each selected potential, the electrode was kept for 5 min, including 2 min for acquisition of a 200-scan spectrum. The ATR/FTIR spectra were recorded at 8 cm^{-1} resolution, at an angle of incidence of 36°, with a Perkin-Elmer model 1760 FTIR spectrometer equipped with a Micro ART unit TR-5 and MCT detector, and represented in absorbance ($-\log(R/R_0)$ or reflectivity ($R \equiv R/R_0$, %) units. Except the spectra at the lowest potentials in the sequences shown in Figures 2 and 5, no smoothing of the spectra was performed.

Solutions of commercial *n*-butyl xanthate ($C_4H_7OS_2K$) recrystallized from acetone were prepared in 0.05 M borate buffer (pH 9.2). Bidistilled water and commercial $Na_2B_4O_7 \cdot 10H_2O$ (pure for analysis) were used. Deaeration was achieved by 1 h of boiling of water with bubbling of high-purity nitrogen. Nitrogen was also bubbled during the following spectroelectrochemical experiments.

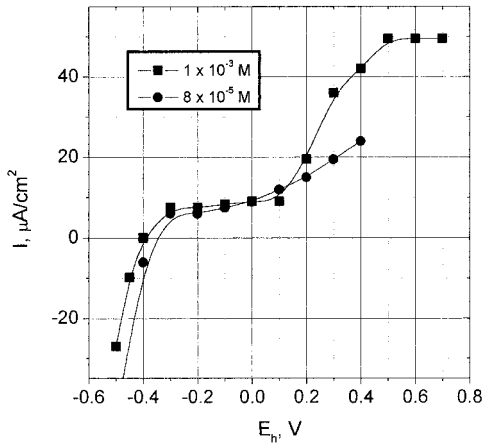

Figure 1. Current−voltage dependencies for a (100) galena electrode in 8×10^{-5} and 1×10^{-3} M solutions of butyl xanthate in deaerated 0.05 M borate buffer, measured simultaneously with the ATR spectra shown in Figures 2 and 5.

Results

The voltammetric curves recorded simultaneously with the ATR spectra of the galena/solution interface are shown in Figure 1. The measurements were performed at applied positive potential bias in 8×10^{-5} M and 1×10^{-3} solutions of *n*-butyl xanthate in a N_2-saturated borate buffer (pH 9.2). Except for the absence of a prepeak, which is developed within the −0.1 to 0 V range in a 1×10^{-3} M solution at a potential scan rate of 5−10 mV/s (not shown), these dependencies are similar to those reported in the literature.[2,3,21,22,27,33,48] Figure 2 shows a sequence of the ATR spectra for a xanthate concentration of 8×10^{-5} M from −0.1 V and on, when the xanthate adsorption is observable. The spectra of the reference bulk compounds are shown in Figure 3. One can see from Figures 2 and 3 that the species adsorbed within the −0.1 to +0.1 V range are similar to bulk lead xanthate $Pb(X)_2$. However, at −0.1 to 0 V the ν_{as}(COC) and ν_{as}(SCS) bands are at 1185 and 1022 cm^{-1}, respectively, while at +0.1 V they shift to 1193 and 1028 cm^{-1}, respectively. Analogous upward shifts for the ν_{as}(COC) and ν_{as}(SCS) bands in the DRIFTS at increasing surface coverage have been reported by Cases and co-workers.[31,32] Since the ATR study of Poling and Leja,[49] an upward shift of the ν_{as}(COC) band has been interpreted in terms of transition from a monocoordinated lead xanthate complex at low surface coverages to bulk lead xanthate in multilayers. However, according to Persson et al.,[23] this shift does not necessary indicate chemisorption. As a matter of fact, such a shift can be produced by the optical effect due to increasing film thickness: it was shown experimentally[27,50] that the ν_{as}(COC) band of polycrystalline lead ethyl xanthate layers deposited from acetone on a Ge internal reflection element shifts from 1190 cm^{-1} at submonolayer coverages to 1210 cm^{-1} for multilayers. To verify this hypothesis, we performed the spectrum simulations using the matrix method of Hansen for isotropic layers[51] for the system "IRE ($n_1 = 2.4$)/galena plate ($n_2 = 3.91$,[52] $d_2 = 10\ \mu$m)/xanthate film/water ($n_4 = 1.26$, $k_4 = 0.036$[53])" in the region of 1300−900 cm^{-1} at an angle of incidence of 36°. The complex permittivity of the isotropic $Pb(X)_2$ film was modeled with a three-oscillator Kramers−Heisenberg formula

$$\hat{\epsilon}(\nu) = \epsilon_\infty + \sum_{j=1}^{3} \frac{S_j \nu_{0j}^2}{\nu_{0j}^2 - \nu^2 + i\nu\gamma}$$

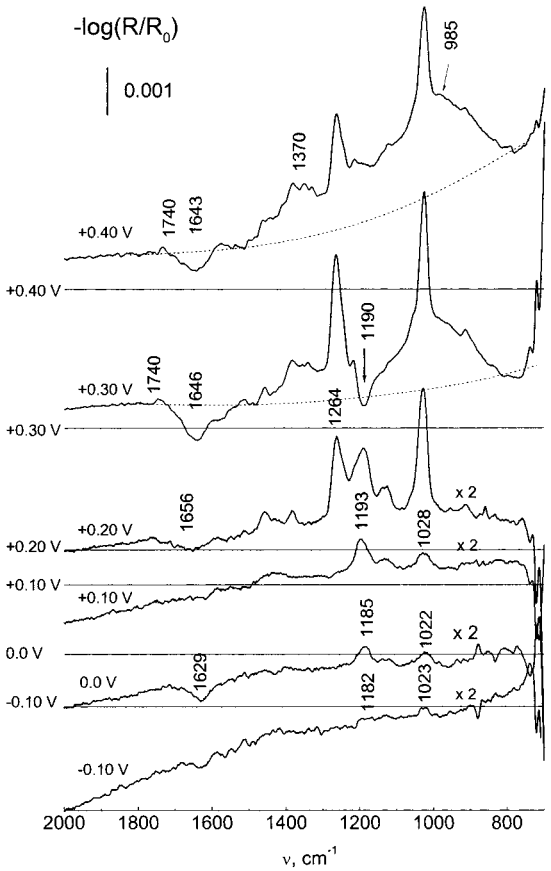

Figure 2. Unpolarized ATR spectra of the "(100) galena/8×10^{-5} M butyl xanthate solution" interface measured during the anodic scan of potential from −0.5 V. The spectrum at a marked potential is referenced to the spectrum at the preceding potential, while the spectrum at −0.1 V is referenced to the spectrum at −0.2 V. The horizontal lines indicate zero absorbance. The dashed lines indicate hole absorption. Note that the ordinate scale for the spectra at −0.1 to +0.2 V is half the indicated scale.

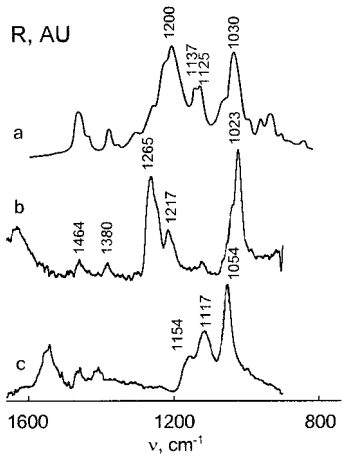

Figure 3. IR spectra of reference compounds: (a) DRIFTS of $Pb(X)_2$ in KBr; (b) ATR of $(X)_2$; (c) ATR of an aqueous solution of KX.

with $\epsilon_\infty = 2.5$, $\gamma_j = 20$ cm^{-1} ($j = 1, 2, 3$), $\nu_{01} = 1200$ cm^{-1}, $S_1 = 0.08$ (ν_{as}(COC)), $\nu_{02} = 1130$ cm^{-1} (ν_s(COC)), $S_2 = 0.04$, $\nu_{03} = 1030$ cm^{-1}, and $S_3 = 0.08$ (ν_{as}(SCS)), which were approximated from the optical constants extracted from the transmission spectrum of lead xanthate pressed in a KBr pellet. Figure 4 shows that the optical effect produces splitting of the ν_{as}(COC) band in the unpolarized ATR spectra. With increasing film thickness from 3 to 100 nm, the spectra are unchanged. A *downward* shift was observed for both the ν_{as}(COC) and

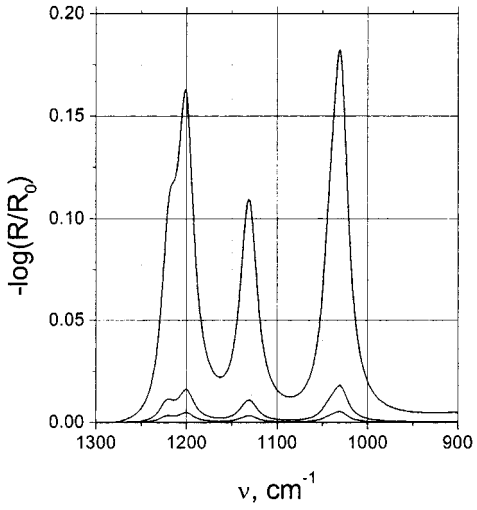

Figure 4. Thickness dependence of simulated ATR spectra of a model organic film at the galena/water interface. The simulation was performed for an angle of incidence of 36°. The optical constants for the IRE, galena, and water were $n_1 = 2.4$, $n_2 = 3.91$, and $n_4 = 1.26$, respectively, and $k_4 = 0.036$. The thickness of the galena layer was taken as $d_2 = 10$ μm. The optical constants of the organic film were chosen to be close to those of lead xanthate but approximated by a three-oscillator Kramers−Heisenberg formula with $\epsilon_\infty = 2.5$, $\gamma_j = 20$ cm^{-1} ($j = 1, 2, 3$), $\nu_{01} = 1200$ cm^{-1}, $S_1 = 0.08$ (ν_{as}(COC)), $\nu_{02} = 1130$ cm^{-1} (ν_s(COC)), $S_2 = 0.04$, $\nu_{03} = 1030$ cm^{-1}, and $S_3 = 0.08$ (ν_{as}(SCS)). The film thickness was 3, 10, and 100 nm from the bottom curve.

ν_{as}(SCS) bands when the film thickness exceeded 1 μm, which is out of the range in question. Similar results were obtained for the film at the Ge/air interface. Hence, the fact that the ν_{as}(COC) band shifts to higher frequencies with increasing adsorbed film thickness cannot be attributed to the optical effect, and even in the case of the cast films on Ge, the lead xanthate structure changes with increasing film thickness. However, the ν_{as}(SCS) band shifted from 1035 to 1019 cm^{-1} in the case of the cast films,[27,50] while it shifts at +0.1 V to *higher* wavenumbers in the ATR spectra shown in Figure 2. Taking into account that the amount of adsorbed xanthate at +0.1 V is on the order of one monolayer (this was approximated using the absorption coefficient determined experimentally[46]) and that the intensity ratio for the ν_{as}(COC) and ν_{as}(SCS) bands differs from that of bulk $Pb(X)_2$ (compare the spectrum at +0.1 V in Figure 2 and spectrum a in Figure 3), one can conclude that, at coverages up to a monolayer, the structure of the adsorbed xanthate complex does differ from that of bulk $Pb(X)_2$.

An additional characteristic band at 1264 cm^{-1} of dixanthogen, $(X)_2$ (Figure 3), is distinct at +0.2 V, close to the reversible potential of reaction 5a. Dixanthogen is still formed at +0.30 V, while $Pb(X)_2$ is almost completely desorbed, as follows from the spectrum referenced to the initial potential of −0.5 V. A closer analysis of the spectra at potentials higher than 0 V reveals a smooth background absorption which increases toward lower wavenumbers (marked by dashed lines at +0.3 and +0.4 V in Figure 2). Such a background has been observed in the cases of the p-Si,[54] Ge,[55] and galena electrodes[29,56] and can be attributed[29] to holes which are generated by anodic decomposition of galena by reaction 4a and accumulated at the interface. Against this background, one can distinguish a small but rather detectable band at 1430 cm^{-1} at +0.1 V and at 1370 cm^{-1} at more anodic potentials. This band can be assigned[29,56] to lead hydroxide (its shift to 1430 cm^{-1} at the initial stage can be due to coadsorbed $Pb(X)_2$). The absorption bands at 1115 and 985 cm^{-1} of lead thiosulfate and a broad band at 950 cm^{-1} of lead sulfite[29] can be seen at +0.3 and +0.4 V. Finally, the spectra measured at +0.3 and +0.4 V reveal a weak band at 1743 cm^{-1}, which can be assigned[31,32] to the carbonyl group of monothoicarbonate ($ROCSO^-$) species.

For comparing with the results of Leppinen et al.[33] and elucidating the effect of xanthate concentration, the ATR spectra were obtained in 1×10^{-3} M xanthate solution (Figure 5). In this case, the xanthate adsorption is detectable at a lower potential (−0.2 V). The ν_{as}(COC) and ν_{as}(SCS) bands of the initial adsorption form of X are analogously red-shifted (to 1180 and 1017 cm^{-1}, respectively) as compared to those of bulk $Pb(X)_2$ (Figure 3). At 0.0 V, the rate of the xanthate adsorption essentially increases, while the ν_{as}(SCS) band of the surface compound shifts to the value of 1030 cm^{-1} characteristic for bulk $Pb(X)_2$. The band at 1265 cm^{-1} of dixanthogen becomes distinct at +0.1 V, which is again close to the thermodynamical value for reaction 5a. From +0.2 to +0.7 V, in contrast to the case of the low xanthate concentration, dixanthogen and lead xanthate only are formed at approximately equal rates, in agreement with the data of Toperi and Tolun[57] (the spectra for $E_h > +0.3$ V are not shown due to their identity to the spectrum at +0.3 V). Hence, the galena autoxidation and the adsorption film decomposition are inhibited.

One can notice some regularities in the changes of the water bending band $\delta_s(H_2O)$ near 1620−1650 cm^{-1} in Figures 2 and 5. The $\delta_s(H_2O)$ band is negative and located at ca. 1625−1630 and 1645−1655 cm^{-1}, respectively, before and after the appearance of dixanthogen at the galena/solution interface. Although the negative intensity can be caused by screening of the water absorption by the organic film, this argument fails to explain the sudden shift of the band with the appearance of dixanthogen. One can conclude that at least a part of the spectral changes in the water absorption are due to reorganization of water molecules near the electrode surface. It has been established[58,59] that water near a nonpolar surface has a high interfacial energy and the chemical potential is equilibrated by an increase in the partial molar volume (a decrease in the water density). Water accomplishes this by forming a more complete ice-like 3D network of self-associated molecules near the surface than in the bulk water. The resulting energetic effect causes H-bonds near a hydrophobic surface to break and may even move water away from the surface, leaving only a thin vapor interlayer (essentially the effect of drying). Conversely, the H-bonded network of water near a surface bearing Lewis sites that can compete with the self-association of water molecules collapses, causing an increase in the chemical potential that accommodates the decreased interfacial energy. This results in an increased density of water. Thus, the degree of self-association and the local density of water scale with the wettability of the surface, which can contribute to the mentioned changes in the band intensity. A higher frequency of the negative $\delta_s(H_2O)$ band observed with deposition of dixanthogen, which is the most hydrophobic derivative of xanthate, can be attributed to the rupture of the strongest H-bonds between the surface and water.

Finally, to elucidate the reversibility of the xanthate adsorption, the galena electrode in 1×10^{-3} M xanthate solution was stepwise anodically polarized from −0.5 up to +0.2 V until a strong absorption by dixanthogen was detected. After that the potential was set back to 0 V, which is close to the open circuit potential (OCP) of galena in the given solution. As seen from Figure 6, the spectrum measured 1 min after switching on 0 V reveals a significant decrease in the total amount of the adsorbed xanthate and almost complete removal of dixanthogen. A further cathodic polarization to −0.2 and −0.4 V results in practically

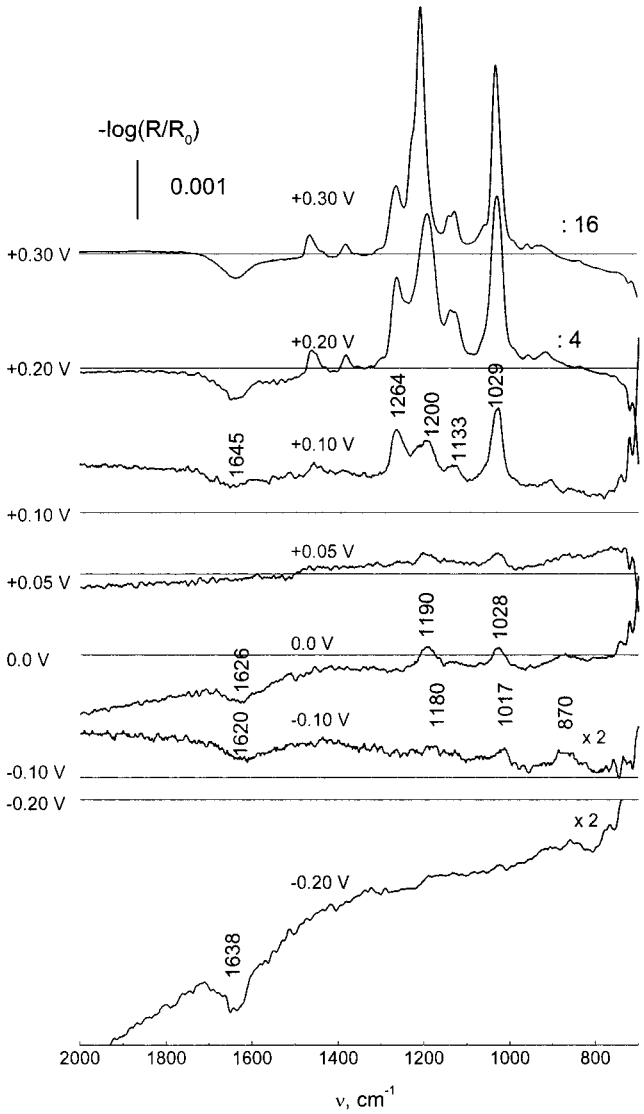

Figure 5. Unpolarized ATR spectra of the "(100) galena/1 × 10^{-3} M butyl xanthate solution" interface measured during the anodic scan of potential from −0.5 V. The spectrum at a marked potential is referenced to the spectrum at the preceding potential, while the spectrum at −0.2 V is referenced to the spectrum at −0.3 V. The horizontal lines indicate zero absorbance. Note that the ordinate scale for the spectra at −0.2, −0.1, +0.2, and +0.3 V differs from the indicated scale.

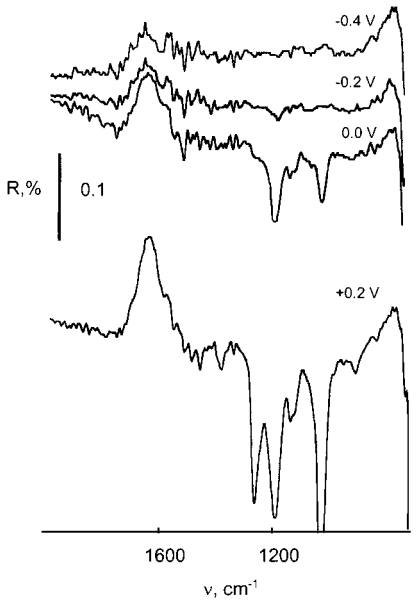

Figure 6. Unpolarized ATR spectra of the "(100) galena/1 × 10^{-3} M butyl xanthate solution" interface measured in deaerated 0.01 M borate at decreasing potential from +0.2 to −0.4 V. The reference potential is −0.5 V. The spectrum at +0.2 V was measured after the electrode potential was increased stepwise as in the case of the spectra shown in Figure 5. The electrode was polarized at 0 V for 1 min before the spectrum acquisition, at the other potentials it was polarized for 2 min.

complete removal of the last $Pb(X)_2$. It follows that $Pb(X)_2$ and especially dixanthogen formed at overpotentials can be easily desorbed at the OCP. This result allows attributing the fact that there were no dixanthogen bands in the ATR spectra obtained by Leppinen et al.[33] to the feature of their technique, which is that, after the anodic polarization at potentials higher than ca. +0.1 V, the electrode was decoupled from the electrochemical equipment and the ATR spectra were measured *at* the OCP.

Discussion

Since the in situ spectra of the galena/solution interface have been obtained for the first time, it is of interest to correlate them with the hypotheses listed in the Introduction.

Contrary to the indirect data,[14,21] physisorbed xanthate, whose spectrum is expected to be similar to that of the solvated anion (Figure 3), is not revealed in the case of the *n*-butyl homologue. Xanthate adsorbed at underpotentials of reaction 2 was found to have a structure somewhat different from that of bulk $Pb(X)_2$, which can be attributed to the contribution of chemisorbed species (eq 1). Consider further xanthate adsorption at the high and low xanthate concentrations separately. In the 1 × 10^{-3} M solution, chemisorption is followed by the formation of bulk $Pb(X)_2$. The reaction involved cannot be described by formulas 4 as no hole absorption is observed. Reaction 3 is ruled out on the basis of the absence of accompanying absorption bands of thiosulfate ion. Therefore, bulk $Pb(X)_2$ is more likely to be formed by reaction 2, which, however, does not produce sulfur-rich sulfide as was previously suggested.[4] This observation can be interpreted within the framework of the Gerisher theory[60,61] of the competition between redox processes and anodic decomposition reactions at the semiconductor/electrolyte interface. Assume that the standard potential for reaction 1 is located in the forbidden gap of galena above the potential of the galena oxidative decomposition. In other words, chemisorption 1 prevents the Fermi level moving toward the valence band edge and, hence, the semiconductor oxidative decomposition. The latter process consumes holes which otherwise would be accumulated at the galena lattice atoms and induce the galena dissolution by reaction 4a. The chemisorbed neutral xanthate species recharges the Helmholtz layer, which is consistent with the observed[22,48] increase in the flatband potential. At the next step, lead xanthate and then lead xanthate and dixanthogen together are formed by reacting the chemisorbed species with lead sulfide

$$PbS + 2(X)_{ads} \rightleftharpoons Pb(X)_2 + S^\circ \qquad (7)$$

$$PbS + 4(X)_{ads} \rightleftharpoons Pb(X)_2 + (X)_2 + S^\circ + 4e \qquad (8)$$

respectively, which are similar to the reactions suggested by Lekki and Chmielewski.[27] Thus, xanthate adsorption at a reagent concentration at which galena oxidative decomposition is suppressed can be described by a series of reactions 1, 7, and 8, which give the overall reactions 2 and 5a.

At 8 × 10^{-5} M, the Fermi level is not pinned within the forbidden band because the diffusion of the xanthate anion

toward the electrode is slower than the rate of the hole generation. As a result, galena is decomposed at +0.1 V by the accumulated holes. The reactions for galena are the same as in the absence of xanthate.[29,56] Namely, a sulfur-rich layer and elemental sulfur are produced by reaction 4a and its bulk analogue at the first step. Lead hydroxide precipitates[29,56] at potentials higher than 0 V, when its solubility product is reached. Afterward lead thiosulfate and lead sulfite are formed by the reactions[29]

$$PbS + S^\circ + 3H_2O + 8h^+ \rightleftharpoons PbS_2O_3 + 6H^+ \quad (9a)$$

$$PbS + 3H_2O + 6h^+ \rightleftharpoons PbSO_3 + 6H^+ \quad (9b)$$

respectively. One can expect that in this regime $Pb(X)_2$ is produced by the precipitation mechanism. Further accumulation of holes at the interface causes decomposition of $Pb(X)_2$ against synthesis of $(X)_2$ at +0.3 V, which can be described by the reaction[24,26]

$$Pb(X)_2 + 2OH^- + 2h^+ \rightleftharpoons Pb(OH)_2 + (X)_2 \ (E^\circ = +0.819 \text{ V}^{18}) \quad (10)$$

whose reversible potential +0.276 V at pH 9.2 is close to the observed value. MTC is not formed in 1×10^{-3} M solution, while at 0.8×10^{-5} M it is formed at +0.4 V when all lead xanthate is mainly decomposed. This suggests that MTC is a product of the anodic decomposition of dixanthogen probably by the reaction

$$(ROCS_2)_2 + 2OH^- + 2h^+ \rightleftharpoons (ROCSO)_2 + 2H^+ \quad (11)$$

There are obvious parallels between the IR spectroscopic data obtained for the 8×10^{-5} M X solution and the galena floatability. According to Trahar,[26] galena ground under reducing conditions starts to float at − 0.1 V in the 2.3×10^{-5} M solution of ethyl xanthate at pH 8, reaching the recovery maximum at +0.2 to +0.3 V, which is followed at +0.35 V by a rapid decrease in floatability. Taking into account the differences in the conditions, one can conclude that the maximal floatability is provided by dixanthogen, rather than by chemisorbed xanthate or lead xanthate. Flotation is canceled with anodic decomposition of lead sulfide into lead hydroxide and lead−sulfur−oxygen compounds and dixanthogen into MTC.

Conclusions

The main conclusion from the in situ ATR/FTIR spectra is that dixanthogen is formed on a galena electrode in deaerated buffer at the potentials which are very close to the reversible potentials for the $X^-/(X)_2$ pair, independently of xanthate concentration. The appearance of dixanthogen makes the surface the most hydrophobic, which can be followed from the changes in the water spectrum. The corresponding potential coincides with the onset of the maximal floatability for galena.[26] Specific adsorption (eq 1), which involves the hole consumption, is the first form of the xanthate adsorption.

Otherwise, the xanthate adsorption on galena at high and low concentrations is different, in agreement with the general conclusion deduced on the basis of the electrochemical data.[27] At high concentrations, the electrochemical oxidation of galena is inhibited by chemisorption 1, which presents the intermediate step for the further formation of lead xanthate and dixanthogen by reactions 7 and 8. At low concentrations, the onset of the formation of bulk $Pb(X)_2$ coincides with the onset of increasing hole absorption, which implies galena oxidative decomposition by reaction 4a and its bulk analogue. In this case, $Pb(X)_2$ forms by the precipitation mechanism (eq 4b), while dixanthogen forms by reaction 5a. At higher potentials, lead xanthate transforms into lead hydroxide, against the synthesis of dixanthogen, which can be described by the overall reaction 10. Finally, dixanthogen decomposes into a dimer of monothiocarbonate (carbonate disulfide) by reaction 11, while galena decomposes into lead sulfite and lead thiosulfate by reactions 9.

Acknowledgment. I thank the Russian Foundation for Basic Research (RFBR) under Grant No. 99-03-32614 for financial support and Profs. V. I. Ryaboi and G. N. Mashevsky (Institute of Ore Processing, Mekhanobr, St. Petersburg, Russia) for stimulation of the FTIR spectroscopic work in flotation.

References and Notes

(1) Finklea, H. O., Ed. *Semiconductor Electrodes (studies in physical and theoretical chemistry)*; Elsevier: Amsterdam, 1988.
(2) Woods, R. In *Flotation*; Fuerstenau, M. C., Ed.; American Institute of Mining and Petroleum Engineers, Inc.: New York, 1976; A. M. Gaudin Memorial Volume, Vol. 1, pp 298−333.
(3) Woods, R. In *Principles of Mineral Flotation. The Wark Symposium*; Jones, M. H., Woodcock, J. T., Eds.; Ausralasian Institute of Mining and Metallurgy (AIMM): Parkville, Victoria, Australia, 1984; pp 91−116.
(4) Woods, R. In *Modern Aspects of Electrochemistry*; Bockris, J. O., Conway, B. E., White, R. E., Eds.; Plenum Press: New York, 1996; Number 29, pp 401−453.
(5) Poling, G. W. In *Flotation*; Fuerstenau, M. C., Ed.; American Institute of Mining and Petroleum Engineers, Inc.: New York, 1976; A. M. Gaudin Memorial Volume, Vol. 1, pp 334−363.
(6) Healy, Th. In *Principles of Mineral Flotation. The Wark Symposium*; Jones, M. H., Woodcock, J. T., Eds.; AIMM: Parkville, Victoria, Australia, 1984; pp 43−56.
(7) Abramov, A. A. *Theoretical basis of optimization of selective flotaiton of sulfide ores*; Nerda: Moscow, 1978 (in Russian).
(8) Klassen, V. I.; Mokrousov, V. A. *Introduction into the theory of flotation*; Gosgortekhizdat: Moscow, 1959 (in Russian).
(9) Wark, I. W. *Report of the Australia and New Zealand Association for the Advancement of Science*, 25th Meeting; Adelaide, 1946; p 23.
(10) Konev, V. A. *Flotation of sulfides*; Nedra: Moscow, 1985 (in Russian).
(11) Shvedov, D. A. *Gorno-Obogat. Zh.* **1936**, *6*, 24 (in Russian).
(12) Shvedov, D. A.; Shorsher, I. N. *Collection of the theoretical and experimental studies of flotation*; Mekhanobr: Leningrad, 1937; Vol. 2, p 2 (in Russian).
(13) Sutherland, K. L.; Wark, J. W. *Principles of Flotation*; AIMM: Melbourne, Australia, 1955.
(14) Forsling, W.; Sun, Z. X. *Int. J. Miner. Process*. **1997**, *51*, 81.
(15) Winter, G. *Rev. Inorg. Chem*. **1980**, *2*, 253.
(16) Glembotski V. A., Anfimova, E. A. *Flotation of oxidized ores of nonferrous metals*; Nedra: Moscow, 1966 (in Russian).
(17) Salamy, S. G.; Nixon, J. C. In *Proceedings of the 2nd International Congress on Surface Activity*; Schulman, J. H., Ed.; Butterworth: London, 1957; Vol. 3, p 369.
(18) Chanturia, V. A.; Vigdergauz, B. E. *Electrochemistry of sulfides*; Nauka: Moscow, 1993; 203 pp (in Russian).
(19) Ndzebet, E.; Schuhmann, D.; Vanel, P. *Electrochim. Acta* **1994**, *39*, 745.
(20) Richadson, P. E.; O'Dell, C. S. *J. Electrochem. Soc*. **1985**, *132*, 1350.
(21) Schuhmann, D.; Guinard-Baticle, A. M.; Lamache, M. *Electrochim. Acta* **1983**, *23*, 79.
(22) Schuhmann, D. Froth Flotation. *Proceedings of the 2nd Latin-American Congress, Concepcion*, Aug 19−23, 1985; Elsevier: Amsterdam, 1988; pp 65−80.
(23) Persson, I.; Persson, P.; Valli, M.; Fozo, S.; Malmensten, B. *Int. J. Miner. Process*. **1991**, *33*, 67.
(24) Guy, P. J.; Trahar, W. J. *Int. J. Miner. Process*. **1984**, *12*, 15.
(25) Tolun, R.; Kitchener, J. A. *Bull.—Inst. Min. Metall*. **1964**, *687*, 313.
(26) Trahar, W.J. In *Principles of Mineral Flotation. The Wark Symposium*; Jones, M. H., Woodcock, J. T., Eds.; AIMM: Parkville, Victoria, Australia, 1984; pp 117−136.
(27) Lekki, J.; Chmielewski, T. *Fizykochem. Probl. Mineralurgii* **1989**, *21*, 127. (in Polish)
(28) Gardner, J. R.; Woods, R. *Austr. J. Chem*. **1977**, *30*, 981.
(29) Chernyshova, I. V. *J. Phys. Chem. B* **2001**, *105*, 8178.

(30) Kakovski, I. K. *Tr. Inst. Gorn. Dela, Akad. Nauk SSSR* **1956**, *3*, 255 (in Russian).
(31) de Donato, Ph.; Cases, J. M.; Kongolo, M.; Michot, L. J.; Burneau, A. *Colloids Surf.* **1990**, *44*, 207.
(32) Cases, J. M.; de Donato, Ph. *Int. J. Miner. Process*. **1991**, *33*, 49.
(33) Leppinen, J. O.; Basilio, C. I.; Yoon, R. H. *Int. J. Miner. Process*. **1989**, *26*, 259.
(34) Golikov, A. *Tsvetn. Metall. (N.Y.)* **1961**, *2*, 19.
(35) Cases, J. M.; Kongolo, M.; de Donato, Ph.; Michot, L. J.; Erre, R. *Int. J. Miner. Process*. **1989**, *28*, 313.
(36) de Donato, Ph.; Cases, J. M.; Kongolo, M. *J. Chim. Phys. Phys.-Chem. Biol.* **1989**, *86*, 409.
(37) Mashevski, G. N. Private communication.
(38) Ahlberg, E.; Broo, A. E. *Int. J. Miner. Process*. **1991**, *33*, 135.
(39) Harris, P. J.; Finkelstein, N. P. *Int. J. Miner. Process*. **1975**, *2*, 77.
(40) Leja, J. *Surface Chemistry of Froth Flotation*; Plenum Press: New York, 1982; p 241.
(41) Mielczarski, J. A.; Mielczarski, E.; Cases, J. M. *Langmuir* **1996**, *12*, 6521.
(42) Mielczarski, J. A.; Cases, J. M.; Alnot, M.; Ehrhardt, J. J. *Langmuir* **1996**, *12*, 2531.
(43) Mielczarski, J. A.; Cases, J. M.; Barres, O. *J. Colloid Interface Sci*. **1996**, *178*, 740.
(44) Weaver, M. J.; Zou, S. In *Spectroscopy for Surface Science*; Clark, R. J. H., Hester, R. E., Eds.; John Wiley and Sons: New York, 1998; Vol. 26, pp 219−272.
(45) Mielczarski, J. A.; Mielczarski, E.; Zachwieja, J.; Cases, J. M. *Langmuir* **1995**, *11*, 2787.
(46) Chernyshova I. V., Tolstoy V. P. *Appl. Spectrosc.* **1995**, *49*, 665.
(47) Peuporte, Th.; Schuhmann, D. *J. Electroanal. Chem*. **1995**, *385*, 9.
(48) Fletcher, S.; Horne, M. D. *Int. J. Miner. Process*. **1991**, *33*, 145.
(49) Poling, G. W.; Leja, J. *J. Phys. Chem*. **1963**, *67*, 2121.
(50) Mielczarski, J.; Nowak, P.; Strojek, J. W. *Pol. J. Chem*. **1980**, *54*, 279.
(51) Hansen, W. N. *J. Opt. Soc. Am*. **1968**, *58*, 380.
(52) Bass, M., Ed. *Handbook of Optics*; Mc-Graw-Hill, Inc.: New York, 1995; Vol. 2, p 33.65.
(53) Palik, E. D. *Handbook of Optical Constants of Solids*; Academic Press: New York, 1998; Vol. 2.
(54) Ozanam, F.; da Fonseca, C.; Rao, A. V.; Chazalviel, J.-N. *Appl. Spectrosc*. **1997**, *51*, 519.
(55) Maroun, F.; Ozanam, F.; Chalzaviel, J.-N. *Surf. Sci.* **1999**, *427*−*428*, 184.
(56) Chernyshova, I. V. *Elektrokhimia* **2001**, *37*, 679 (in Russian).
(57) Toperi, D.; Tolun, R. *Trans.*—*Inst. Min. Metall., C* **1969**, *78*, C191.
(58) Vogler, E. A. *Adv. Colloid Interface Sci.* **1998**, *74*, 69.
(59) Richmond, G. L. *Langmuir* **1997**, *13*, 4804.
(60) Gerischer, H. *Semiconductors Electrochemistry. Physical Chemistry*; Academic Press: New York, 1970; p 463.
(61) Gerischer, H. *Surf. Sci*. **1969**, *13*, 265.